

20 **Abstract**

21 A new coronavirus SARS-CoV-2, recently discovered in Wuhan, China, has caused over 74000
22 infection cases and 2000 deaths. Due to the rapidly growing cases and the unavailability of
23 specific therapy, there is a desperate need for vaccines to combat the epidemic of SARS-CoV-2. In
24 the present study, we performed an in silico approach based on the available virus genome to
25 identify the antigenic B-cell epitopes and human-leukocyte-antigen (HLA) restricted T-cell
26 epitopes. A total of 61 B-cell epitopes were initially identified, 19 of which with higher potential
27 immunogenicity were used for vaccine design. 499 T-cell epitopes were predicted that showed
28 affinity with the 34 most popular HLA alleles in Chinese population. Based on these epitopes, 30
29 vaccine candidates were designed and inspected against safety risks, including potential toxicity,
30 human homologous, pharmaceutical peptides and bioactive peptides. Majority of vaccine peptides
31 contained both B-cell and T-cell epitopes, which may interact with the most prevalent HLA alleles
32 accounting for ~99% of Chinese population. Docking analysis showed stable hydrogen bonds of
33 epitopes with their corresponding HLA alleles. In conclusion, these putative antigenic peptides
34 may elicit the resistance response to the viral infection. In vitro and in vivo experiments are
35 required to validate the effectiveness of these peptide vaccine.

36

37 **Keywords:** SARS-CoV-2, epitope, immunoinformatics, vaccine

38 **1. Introduction**

39 Since December 2019, Wuhan City, Hubei Province, China has become the center of an outbreak
40 of viral lung infections caused by a new type of coronavirus, SARS-CoV-2 (previously named
41 2019-nCoV by the World Health Organization) (Gorbalenya, 2020; Joseph T Wu*, 2020;
42 Organization, 2020; Perlman, 2020). The outbreak has so far infected over 74000 patients, and has
43 spread to approximately 30 countries/regions worldwide. Comparisons of the genome sequences
44 of SARS-CoV-2 with other virus has shown 79.5% and 96% similarities at nucleotide level to
45 SARS-CoV and bat coronaviruses, respectively (Zhou et al., 2020), which suggested its probable
46 origin in bats (Benvenuto et al., 2020). The main clinical manifestations of SARS-CoV-2 patients
47 are fever ($\geq 38^{\circ}\text{C}$), dry cough, low or normal peripheral white blood cell count, and low
48 lymphocyte count, known as novel coronavirus-infected pneumonia (NCIP) or coronavirus
49 disease 2019 (COVID19) (Huang et al., 2020).

50 Currently, there is no approved therapeutics or vaccines available for the treatment of
51 COVID19 (Chen et al.). Due to lack of anti-viral drugs or vaccines, control measures have been
52 relying on the rapid detection and isolation of symptomatic cases (Chen et al.). In this context, a
53 safe and efficacious vaccine is urgently required. Traditional approaches for developing vaccines
54 waste much time in isolating, inactivating and injecting the microorganisms (or portions of them)
55 that cause disease. Fortunately, computation-based method enable us to start from analysis of viral
56 genome, without the need to grow pathogens and therefore speeding up the entire process.
57 Complete genome sequencing of SARS-CoV-2 has finished and paved the way for the vaccine
58 development (Chen et al.). The genome of SARS-CoV-2 encodes the spike protein, the membrane
59 protein, the envelope protein, the nucleocapsid protein and a few replication and

60 transcription-related enzymes. Given the lack of repairing mechanism of RNA virus replicase
61 complex, mutations are prone to occur during virus replication. The 4% nucleotide difference of
62 the virus isolated from Rhinolophus to that from human suggests that SARS-CoV-2 mutates
63 rapidly to achieve the host conversion (Jiayuan Chen, 2020). Like SARS-CoV, SARS-CoV-2 uses
64 its receptor binding domain (RBD) on the spike protein to bind to the host's
65 angiotensin-converting enzyme 2 (ACE2) (Chen et al.; Dong et al., 2020; Tian et al., 2020; Zhou
66 et al., 2020). In terms of binding capacity, the RBD of SARS-CoV-2 is much stronger than
67 SARS-CoV and is considered to be between HKU3-4 which cannot bind to ACE2 receptor and
68 rSHC014 which presents the largest binding energy (Gralinski and Menachery, 2020; Wrapp et al.,
69 2020; Zhao et al., 2020). Consequently, the SARS-CoV-2 vaccine can be developed targeting the
70 structural proteins, and in particular, the RBD region, following the strategy for the SARS-CoV
71 vaccine development (Babcock et al., 2004; Buchholz et al., 2004; He et al., 2005; Saif, 1993;
72 Tian et al., 2020).

73 An ideal vaccine may contain both B-cell epitopes and T-cell epitopes, with combination of
74 which vaccine is able to either induce specific humoral or cellular immune against pathogens
75 efficiently (Purcell et al., 2007). Since the development of a peptide vaccine against the virus
76 causing foot-and-mouth disease (Adam et al., 1978), the establishment of peptide synthesis
77 method by Lerner et al. (Lerner et al., 1981), along with the advent of a peptide vaccine design
78 combining T-cell and B-cell epitopes, has accelerated the vaccine development. In the present
79 study, we followed this in silico approach to identify the potential B-cell and T-cell epitope(s)
80 from the spike, envelope and membrane proteins that could be used as promising vaccines against
81 SARS-CoV-2.

82

83 **2. Materials and Methods**

84 **2.1. Data retrieval**

85 The genome sequence of SARS-CoV-2 isolate Wuhan-Hu-1 was retrieved from the NCBI
86 database under the accession number MN908947. Gene and protein sequences were acquired
87 according to the annotation. In particular, the RBD region for the spike protein was referred to as
88 the fragment from 347 to 520 amino acid (aa) (Lu et al., 2020).

89 **2.2. B-cell epitope prediction**

90 The online tool in IEDB (Immune-Epitope-Database And Analysis-Resource) was used for the
91 analysis of the conserved regions of the candidate epitopes (Vita et al., 2015). Prediction of linear
92 B-cell epitopes was performed through Bepipred software (Jespersen et al., 2017). The antigenic
93 sites were determined with Kolaskar method (Chen et al., 2007). The surface accessible epitopes
94 were predicted by Emini tool (Almofti et al., 2018).

95 **2.3. T-cell epitope prediction**

96 The sequences of structural proteins were split into small fragments with a length of 9aa; their
97 binding affinity with the 34 most prevalent HLA alleles (>1% in the Chinese population according
98 to data obtained from the website for China Marrow Donor Program (CMDP)) was predicted
99 using netMHCpan (Hoof et al., 2009) and our in-house prediction software iNeo-Pred,
100 respectively. iNeo-Pred was trained on a large immune-peptide dataset, and achieved a better
101 performance in predicting binding affinity of epitopes to specific HLA alleles. Only the epitopes

102 predicted by both tools were selected. Next, for each epitope, a HLA score was calculated based
103 on the frequencies of binding HLA alleles in Chinese population, which will be used as metrics to
104 select better candidates for downstream analysis.

105 **2.4. Vaccine peptide design**

106 The vaccine peptides were designed by our in-house tool iNeo-Design. First, the selected B-cell
107 epitopes and their adjacent T-cell epitopes were bridged to form candidate peptides with length no
108 more than 30aa. Meanwhile, to facilitate the peptide synthesis, vaccine peptide sequences were
109 optimized based on their hydrophobicity and acidity. To minimize the safety risk, peptides that
110 contained toxicity potential, human homologous region (full-length matches and identity > 95%),
111 or bioactive peptide were discarded.

112 Besides the vaccine peptides containing both B-cell epitopes and T-cell epitopes,
113 iNeo-Design also utilized all predicted T-cell epitopes to generate T-cell epitopes-only vaccine
114 peptides. For each vaccine candidate, the epitope counts and HLA score reflecting the population
115 coverage were calculated. Vaccine candidates with the higher epitope counts and HLA score were
116 considered to be preferable for the downstream analysis.

117 **2.5. Structural analysis**

118 The online server swiss-model was used to predict the 3D protein structures of viral proteins and
119 HLA molecules (Waterhouse et al., 2018). The online server PEP_FOLD was used to predict
120 T-cell epitopes' structures (Lamiable et al., 2016). To display the interaction between T-cell
121 epitopes and HLA molecules, T-cell epitope models were docked to HLA molecules using
122 MDockPep (Xu et al., 2018). All predicted structures or models were decorated and displayed by

123 the open source version of pymol program (<https://github.com/schrodinger/pymol-open-source>).

124 **Ethics**

125 N/A.

126 **Data availability**

127 N/A.

128

129 **3. Results and Discussion**

130 **3.1. Prediction of B-cell epitopes**

131 During the immune response against viral infection, B-cell takes in viral epitopes to recognize
132 viruses and activates defense responses. Recognition of B-cell epitopes depends on antigenicity,
133 accessibility of surface and predictions of linear epitope (Fieser et al., 1987). A total of 61 B-cell
134 epitopes were predicted, which seemed preferentially located within certain regions of each gene
135 (Figure 1; Figure 2; Table S1). Only 19 epitopes were exposed on the surface of the virion and had
136 a high antigenicity score, indicating their potentials in initiating immune response. Therefore, they
137 were considered to be promising vaccine candidates against B-cells. Among the 19 epitopes, 17
138 were longer than 14 residues and located in the spike protein that contained RBD and functioned
139 in host cell binding (Table 1). The average Emini score for the 19 epitopes was 2.744, and the
140 average for Kolaskar (antigenicity) score was 1.015. Two epitopes were located within the RBD
141 region, while the one with the highest Kolaskar score (1.059), 1052-FPQSAPH-1058, was located
142 at position 1052aa of the spike protein.

143 **3.2. Prediction of T-cell epitopes**

144 The immune response of T-cell is considered as a long lasting response compared to B-cell where
145 the antigen might easily escape the antibody memory response (Black et al., 2010). Moreover, the
146 CD8+ T and CD4+ T-cell responses play a major role in antiviral immunity. It is therefore
147 important to design vaccines that can induce T-cell's immune response (Sesardic, 1993). A total of
148 499 T-cell epitopes were predicted on the spike protein (378 epitopes), the membrane protein (90
149 epitopes) and the envelop protein (31 epitopes); 48 of the 378 epitopes for the spike protein were
150 located in the RBD region (Figure 1; Table 2; Table S2). There is no preference in certain genes or
151 regions for T-cell epitope generation; no biased distribution of T-cell epitopes among HLA types
152 were observed either. Among all T-cell epitopes, the epitope 869-MIAQYTSAL-877 in the spike
153 protein was predicted to be able to bind to 17 HLA alleles. Most of the HLA alleles included in the
154 present study were covered by these vaccine candidates, which suggested a wide population
155 coverage.

156 In terms of the distribution of the predicted epitopes against different HLA haplotypes, no
157 significant differences were observed among different HLA haplotypes (Table S3). There were
158 287, 208 and 195 epitopes predicted to be able to bind to HLA-A, HLA-B and HLA-C haplotypes,
159 respectively. For the most popular five HLA types (HLA-A*11:01, HLA-A*24:02, HLA-C*07:02,
160 HLA-A*02:01 and HLA-B*46:01), the counts for epitopes with binding affinity were 51, 49, 115,
161 48 and 58.

162 **3.3. Multi-epitope vaccine design**

163 Based on the 19 B-cell epitopes and their 121 adjacent T-cell epitopes, 17 candidate vaccine

164 peptides that contained both B-cell and T-cell epitopes were generated by our in-house software
165 iNeo-Design. Most of the 17 candidate vaccine peptides contained one B-cell epitopes, except for
166 AVEQDKNTQEVFAQVKQIYKTPPIKDFGG, which involved two B-cell epitopes and eight
167 T-cell epitopes, and AKNLNESLIDLQELGKYEQYIKWPWYIWKK, which contained two
168 B-cell epitopes and 6 T-cell epitopes. By comparison, the vaccine peptide
169 FKNLREFVFKNIDGYFKIYSKHTPINLV had the largest count of T-cell epitopes, whereas the
170 vaccine peptide SYGFQPTNGVGYQPYRVVLSFELLHAPAT showed the highest HLA score,
171 indicating their wide population coverage and promising efficacy.

172 In addition to the vaccine candidates involved both B-cell and T-cell epitopes, we also
173 analysed the entire 499 core T-cell epitopes to generate another 102 vaccine peptides containing
174 T-cell epitopes only. Based on both the epitope counts and HLA score, we eventually selected 13
175 T-cell epitopes-only vaccine peptides.

176 Taken together, a total of 30 peptide vaccine candidates were designed (Table 3). 26 of them
177 were from the spike protein, two from the membrane protein and two from the envelop protein.
178 Five peptides were located in the RBD region, indicating they were likely to induce the production
179 of neutralizing antibody. The 30 vaccine peptides covered all structural proteins that may induce
180 immune response against SARS-CoV-2 in theory; and the multi-peptide strategy we applied would
181 better fit the genetic variability of the human immune system and reduce the risk of pathogen's
182 escape through mutation (Skwarczynski and Toth, 2016).

183 **3.4. Interaction of predicted peptides with HLA alleles**

184 To further inspect the binding stability of T-cell epitopes against HLA alleles, the T-cell epitopes

185 involved in the above designed vaccine peptides were selected to conduct an interaction analysis.
186 Figure 3 illustrated the docking results against the most popular HLA types for the two epitopes
187 from vaccines peptide 25 and 27 (Table 3; Table 4), which showed relatively higher HLA score.
188 The MDockPep scores were between -148 ~ -136, indicating that the predicted crystal structures
189 were stable. All epitopes were docked inside the catalytic pocket of the receptor protein. In
190 particular, the epitope 1220-FIAGLIAIV-1228 from the spike protein possessed 2-5 stable
191 hydrogen bonds with the HLA alleles; the epitope 4-FVSEETGTL-12 from the envelop protein
192 possessed 4-5 stable hydrogen bonds (Table 4). Taken together, the epitopes included in our
193 vaccine peptides can interact with the given HLA alleles by in silico prediction.

194

195 **4. Conclusions**

196 Vaccine design using an in silico prediction method is highly appreciated as it selects specific
197 epitopes in proteins than conventional methods. In the present study, this reverse vaccinology
198 approach was adopted to identify surface-exposed peptides, instead of targeting the whole
199 pathogen which is obviously less efficient and effective. Immunogenic regions of antigenic
200 epitopes of all proteins encoded by SARS-CoV-2 were screened to identify potential vaccine
201 candidates. As a result, 17 vaccine peptides involving both T-cell epitopes and B-cell epitopes as
202 well as 13 vaccine peptides involving T-cell epitopes only were successfully designed. These
203 multi-epitope vaccines provided excellent candidates for the development of vaccines against
204 SARS-CoV-2. Various formulation of vaccine can be rapidly manufactured, such as peptide, DNA
205 and mRNA. However in vitro and in vivo trials are required to achieve the effectiveness of these

206 vaccine peptides.

207

208 **Acknowledgements**

209 This work was supported by Zhejiang Provincial Natural Science Foundation of China.

210

211 **Author contributions**

212 SC and FM conceived and designed the project. MQ, SZ, KL, RC, YS, KW, XZ and SZ analysed

213 the data. YF and YL wrote the initial draft. All authors revised and approved the final manuscript.

214

215 **Declarations of interest: none**

216

217 **References**

218 Adam, K.-H., Kaaden, O., Strohmaier, K., 1978. Isolation of immunizing cyanogen

219 bromide-peptides of foot-and-mouth disease virus. Biochemical and biophysical research

220 communications 84, 677-683.

221 Almofti, Y.A., Abd-elrahman, K.A., Gassmallah, S.A.E., Salih, M.A., 2018. Multi Epitopes

222 Vaccine Prediction against Severe Acute Respiratory Syndrome (SARS) Coronavirus Using

223 Immunoinformatics Approaches. American Journal of Microbiological Research 6, 94-114.

224 Babcock, G.J., Esshaki, D.J., Thomas, W.D., Ambrosino, D.M., 2004. Amino acids 270 to 510
225 of the severe acute respiratory syndrome coronavirus spike protein are required for interaction
226 with receptor. *J Virol* 78, 4552-4560.

227 Benvenuto, D., Giovanetti, M., Ciccozzi, A., Spoto, S., Angeletti, S., Ciccozzi, M., 2020. The
228 2019-new coronavirus epidemic: evidence for virus evolution. *Journal of Medical Virology*.

229 Black, M., Trent, A., Tirrell, M., Olive, C., 2010. Advances in the design and delivery of peptide
230 subunit vaccines with a focus on toll-like receptor agonists. *Expert review of vaccines* 9,
231 157-173.

232 Buchholz, U.J., Bukreyev, A., Yang, L.J., Lamirande, E.W., Murphy, B.R., Subbarao, K.,
233 Collins, P.L., 2004. Contributions of the structural proteins of severe acute respiratory
234 syndrome coronavirus to protective immunity. *P Natl Acad Sci USA* 101, 9804-9809.

235 Chen, J., Liu, H., Yang, J., Chou, K.-C., 2007. Prediction of linear B-cell epitopes using amino
236 acid pair antigenicity scale. *Amino acids* 33, 423-428.

237 Chen, Y., Liu, Q., Guo, D., Emerging coronaviruses: genome structure, replication, and
238 pathogenesis. *Journal of Medical Virology*.

239 Dong, N., Yang, X., Ye, L., Chen, K., Chan, E.W.-C., Yang, M., Chen, S., 2020. Genomic and
240 protein structure modelling analysis depicts the origin and infectivity of 2019-nCoV, a new
241 coronavirus which caused a pneumonia outbreak in Wuhan, China. *bioRxiv*.

242 Fieser, T.M., Tainer, J.A., Geysen, H.M., Houghten, R.A., Lerner, R.A., 1987. Influence of
243 protein flexibility and peptide conformation on reactivity of monoclonal anti-peptide antibodies

244 with a protein alpha-helix. Proceedings of the National Academy of Sciences 84, 8568-8572.

245 Gorbalenya, A.E., 2020. Severe acute respiratory syndrome-related coronavirus – The
246 species and its viruses, a statement of the Coronavirus Study Group. bioRxiv,
247 2020.2002.2007.937862.

248 Gralinski, L.E., Menachery, V.D., 2020. Return of the Coronavirus: 2019-nCoV. Viruses 12,
249 135.

250 He, Y.X., Lu, H., Siddiqui, P., Zhou, Y.S., Jiang, S.B., 2005. Receptor-binding domain of
251 severe acute respiratory syndrome coronavirus spike protein contains multiple
252 conformation-dependent epitopes that induce highly potent neutralizing antibodies. J Immunol
253 174, 4908-4915.

254 Hoof, I., Peters, B., Sidney, J., Pedersen, L.E., Sette, A., Lund, O., Buus, S., Nielsen, M., 2009.
255 NetMHCpan, a method for MHC class I binding prediction beyond humans. Immunogenetics
256 61, 1.

257 Huang, C., Wang, Y., Li, X., Ren, L., Zhao, J., Hu, Y., Zhang, L., Fan, G., Xu, J., Gu, X., 2020.
258 Clinical features of patients infected with 2019 novel coronavirus in Wuhan, China. The
259 Lancet.

260 Jespersen, M.C., Peters, B., Nielsen, M., Marcatili, P., 2017. BepiPred-2.0: improving
261 sequence-based B-cell epitope prediction using conformational epitopes. Nucleic acids
262 research 45, W24-W29.

263 Jiayuan Chen, J.S., Tungon Yau ,Chang Liu , Xin L, Qiang Zhao, Jishou Ruan , Gao Shan.,

- 264 2020. Bioinformatics analysis of the Wuhan 2019 human coronavirus genome.
- 265 Joseph T Wu*, K.L., Gabriel M Leung, 2020. Nowcasting and forecasting the potential
266 domestic and international spread of the 2019-nCoV outbreak originating in Wuhan, China: a
267 modelling study. *The Lancet*.
- 268 Lamiable, A., Thevenet, P., Rey, J., Vavrusa, M., Derreumaux, P., Tuffery, P., 2016.
269 PEP-FOLD3: faster de novo structure prediction for linear peptides in solution and in complex.
270 *Nucleic Acids Res* 44, W449-454.
- 271 Lerner, R.A., Green, N., Alexander, H., Liu, F.-T., Sutcliffe, J.G., Shinnick, T.M., 1981.
272 Chemically synthesized peptides predicted from the nucleotide sequence of the hepatitis B
273 virus genome elicit antibodies reactive with the native envelope protein of Dane particles.
274 *Proceedings of the National Academy of Sciences* 78, 3403-3407.
- 275 Lu, R., Zhao, X., Li, J., Niu, P., Yang, B., Wu, H., Wang, W., Song, H., Huang, B., Zhu, N., Bi,
276 Y., Ma, X., Zhan, F., Wang, L., Hu, T., Zhou, H., Hu, Z., Zhou, W., Zhao, L., Chen, J., Meng, Y.,
277 Wang, J., Lin, Y., Yuan, J., Xie, Z., Ma, J., Liu, W.J., Wang, D., Xu, W., Holmes, E.C., Gao,
278 G.F., Wu, G., Chen, W., Shi, W., Tan, W., 2020. Genomic characterisation and epidemiology
279 of 2019 novel coronavirus: implications for virus origins and receptor binding. *Lancet*.
- 280 Organization, W.H., 2020. Surveillance case definitions for human infection with novel
281 coronavirus (nCoV): interim guidance v1, January 2020. , in: Organization, W.H. (Ed.). *World
282 Health Organization*, Geneva.
- 283 Perlman, S., 2020. Another Decade, Another Coronavirus. *New England Journal of Medicine*.

- 284 Purcell, A.W., McCluskey, J., Rossjohn, J., 2007. More than one reason to rethink the use of
285 peptides in vaccine design. *Nat Rev Drug Discov* 6, 404-414.
- 286 Saif, L.J., 1993. Coronavirus Immunogens. *Vet Microbiol* 37, 285-297.
- 287 Sesardic, D., 1993. Synthetic peptide vaccines. *Journal of medical microbiology* 39, 241-242.
- 288 Skwarczynski, M., Toth, I., 2016. Peptide-based synthetic vaccines. *Chemical science* 7,
289 842-854.
- 290 Tian, X., Li, C., Huang, A., Xia, S., Lu, S., Shi, Z., Lu, L., Jiang, S., Yang, Z., Wu, Y., 2020.
291 Potent binding of 2019 novel coronavirus spike protein by a SARS coronavirus-specific human
292 monoclonal antibody. *bioRxiv*.
- 293 Vita, R., Overton, J.A., Greenbaum, J.A., Ponomarenko, J., Clark, J.D., Cantrell, J.R., Wheeler,
294 D.K., Gabbard, J.L., Hix, D., Sette, A., 2015. The immune epitope database (IEDB) 3.0.
295 *Nucleic acids research* 43, D405-D412.
- 296 Waterhouse, A., Bertoni, M., Bienert, S., Studer, G., Tauriello, G., Gumienny, R., Heer, F.T.,
297 de Beer, T.A.P., Rempfer, C., Bordoli, L., Lepore, R., Schwede, T., 2018. SWISS-MODEL:
298 homology modelling of protein structures and complexes. *Nucleic Acids Res* 46, W296-W303.
- 299 Wrapp, D., Wang, N., Corbett, K.S., Goldsmith, J.A., Hsieh, C.-L., Abiona, O., Graham, B.S.,
300 McLellan, J.S., 2020. Cryo-EM Structure of the 2019-nCoV Spike in the Prefusion
301 Conformation. *bioRxiv*, 2020.2002.2011.944462.
- 302 Xu, X., Yan, C., Zou, X., 2018. MDockPeP: An ab-initio protein-peptide docking server. *Journal*
303 *of computational chemistry* 39, 2409-2413.

304 Zhao, Y., Zhao, Z., Wang, Y., Zhou, Y., Ma, Y., Zuo, W., 2020. Single-cell RNA expression
305 profiling of ACE2, the putative receptor of Wuhan 2019-nCov. bioRxiv.

306 Zhou, P., Yang, X.-L., Wang, X.-G., Hu, B., Zhang, L., Zhang, W., Si, H.-R., Zhu, Y., Li, B.,
307 Huang, C.-L., 2020. Discovery of a novel coronavirus associated with the recent pneumonia
308 outbreak in humans and its potential bat origin. bioRxiv.

309

310

311

312 **Figure legends**

313 **Fig. 1.** Distribution of B-cell and T-cell epitopes. The outermost circle (light blue) stands for the
314 T-cell epitope count. The 2nd outer circle stands for Emini (in red) and Kolaskar (in green) score
315 used to evaluate the B-cell epitopes. The 3rd circle marked the name of the viral proteins. The
316 4th-6th circles stands for HLA-A (in blue), HLA-B (in green), and HLA-C (in yellow) scores; the
317 points closer to the center indicates a lower score.

318

319 **Fig. 2.** Locations of the recognized B cell epitopes on the viral spike protein (a), envelop protein
320 (b) and membrane protein (c). The transparent cartoon models display the predicted 3D structure;
321 the colorful balls marks the position of the recognized epitopes.

322

323 **Fig. 3.** Interaction between the predicted peptides (by yellow sticks) and different HLA alleles (by
324 green cartoons). Amino acids were labeled adjacent to the contact sites. Table 3 displays the
325 detailed docking information.

326

327

328

329

330

331

332

333

334

335

336

337

338

339

Table 1. B-cell epitope candidates

Epitope	Protein	Start	End	Peptide	Emini	Kolaskar
B1	Spike	19	43	TTRTQLPPAYTNSFTRGVYYDPKVF	6.424	1.028
B2	Spike	90	99	VYFASTEKSN	1.573	1.019
B3	Spike	206	209	KHTP	2.463	1.002
B4	Spike	405	430	DEVQRQIAPGQTGKIADYNYKLPDDFT	5.81	1.001
B5	Spike	494	507	SYGFQPTNGVGYQP	1.553	1.02
B6	Spike	671	688	CASYQTQTNSPRRARSVA	3.531	1.027
B7	Spike	771	782	AVEQDKNTQEVF	2.342	1.011
B8	Spike	787	799	QIYKTPPIKDFGG	1.465	1.006
B9	Spike	805	816	ILPDPSKPSKRS	4.69	1.019
B10	Spike	1052	1058	FPQSAPH	1.381	1.059
B11	Spike	1068	1091	VPAQEKNFTTAPAICHGKAHFPR	1.063	1.03
B12	Spike	1108	1123	NFYEPQIITDNTFVS	1.039	1.007

B13	Spike	1135	1151	NTVYDPLQPELDSFKEE	6.183	1.011
B14	Spike	1153	1172	DKYFKNHTSPDVLGDISGI	1.399	1.007
B15	Spike	1190	1193	AKNL	1.087	1.005
B16	Spike	1203	1209	LGKYEQY	2.512	1.035
B17	Spike	1255	1265	KFDEDDSEPVL	2.654	1.003
B18	Spike	63	70	KNLNSSRV	3.471	1.002
B19	Spike	173	176	SRTL	1.504	1.011

Note: Epitopes B4 and B5 are located within the RBD region.

Table 2. Distribution of T-cell epitopes among three structural proteins

Protein	Count of T-cell Epitope	No. of epitope per residue	Epitope overage	HLA Types Count
Spike	378	0.297	93.01%	33
Membrane	90	0.405	96.00%	31
Envelop	31	0.413	94.14%	32

Table 3. Candidate vaccine peptides

Peptide	Protein	Start	End	Vaccine peptide	Count of T Epitopes	Count of B Epitopes	HLA Score
P1	Spike	19	46	TTRTQLPPAYTNSFTRGVYYPDKVFRSS	10	1	1.086
P2	Spike	75	99	GTKRFDNPVLPFNDGVYFASTEKSNK	6	1	1.143
P3	Spike	118	143	LIVNNATNVVIKVCEFQFCNDPFLGVKK	7	0	1.179
P4	Spike	142	170	GVYYHKNNKSWMESEFRVYSSANNCTFEY	10	0	1.664
P5	Spike	186	209	FKNLREFVFKNIDGYFKIYSKHTP	8	1	1.264
P6	Spike	258	279	WTAGAAAYYVGYLQPRTFLLKYKKKKK	10	0	1.115
P7	Spike	310	337	KGIYQTSNFRVQPTESIVRFPNITNLCP	10	0	1.012
P8 *	Spike	357	386	RISNCVADYSVLYNSASFSTFKCYGVSPTK	8	0	1.318
P9 *	Spike	405	433	DEVQRQIAPGQTGKIADYNYKLPDDFTGKKK	7	1	0.928
P10 *	Spike	448	472	NYNYLYRLFRKSNLKPFRDISTEI	7	0	1.625
P11 *	Spike	478	505	TPCNGVEGFNCYFPLQSYGFQPTNGVGYKK	7	0	1.413
P12 *	Spike	494	523	SYGFQPTNGVGYQPYRVVVLSFELLHAPAT	10	1	1.581

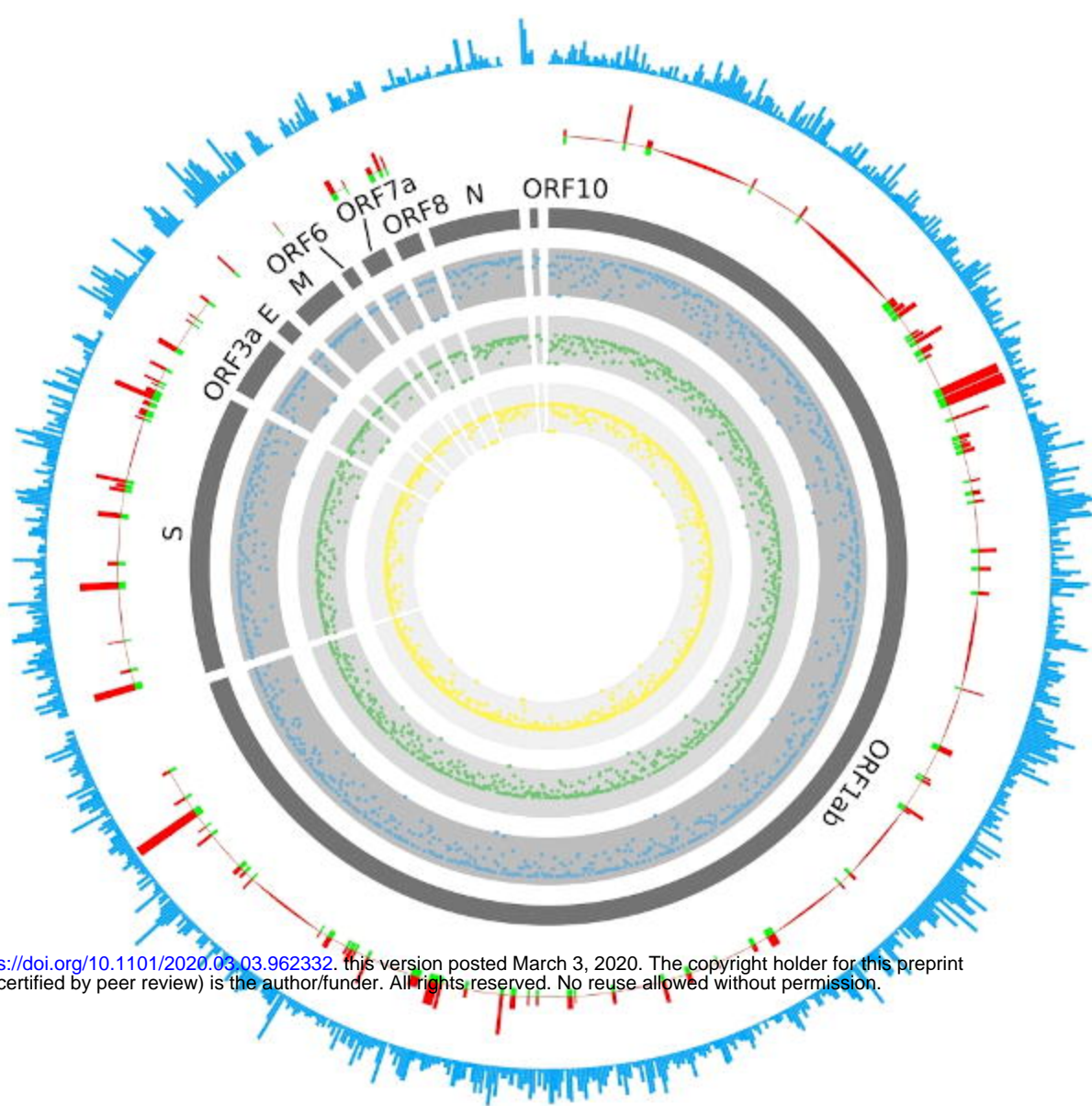
P13	Spike	625	652	HADQLTPTWRVYSTGSNVFQTRAGCLIG	8	0	1.214
P14	Spike	671	699	CASYQTQTNSPRRARSVASQSIIAYTMSL	8	1	1.234
P15	Spike	771	799	AVEQDKNTQEVFAQVKQIYKTPPIKDFGGK	8	2	0.952
P16	Spike	805	833	ILPDPSKPSKRSFIEDLLFNKVTLADAGFK	7	1	1.068
P17	Spike	896	923	IPFAMQMAYRFNGIGVTQNVLYENQKLI	7	0	1.625
P18	Spike	965	991	QLSSNFGAISSVLNDILSRDKVEAEVKKK	9	0	1.012
P19	Spike	1052	1073	FPQSAPHGVVFLHVTVVPAQEK	8	1	1.532
P20	Spike	1068	1096	VPAQEKNFHTTAPAICHGKAHFPREGVVFV	4	1	0.402
P21	Spike	1095	1123	FVSNNGTHWFVTQRNFYEPQIITDNTFVSK	8	1	1.236
P22	Spike	1135	1155	NTVYDPLQPELDSFKEELDKYKKKKK	2	1	0.254
P23	Spike	1153	1181	DKYFKNHTSPDVDLGDISGINASVVNIQKK	5	1	0.322
P24	Spike	1190	1217	AKNLNESLIDLQELGKYEYIKWPWYIWKK	6	2	0.659
P25	Spike	1216	1245	IWLGFIAGLIAIVMVTIMLCKKKKKKKKKK	5	0	1.394
P26	Spike	1236	1265	KKKKCCSCLKGCCSCGSCCKFDEDDSEPVL	4	1	0.520

P27	Envelop	4	33	FVSEETGTLIVNSVLLFLAFVVFLKKKKKK	11	0	1.133
P28	Envelop	45	70	NIVNVSLVKPSFYVYSRVKLNSSRV	9	1	1.455
P29	Membrane	122	150	VPLHGTILTRP LLESELVIGAVILRGHLRK	9	0	1.508
P30	Membrane	173	201	SRTLSYYKLGASQRVAGDSGFAAYSRYRI	6	1	0.902

Note: Peptide labeled by asterisks (*) are located within the RBD region.

Table 4. Docking results for T-cell epitope P25 and P27 against three HLA types

Panel in	Protein	Start	Epitope	HLA type	HLA Score	ITScorePeP	Contact residues
Fig. 3							
a	Spike	1220	FIAGLIAIV	HLA-A*02:01	0.123	-144.2	PHE-1, GLY-4, LEU-5, ILE-6, ALA-7
b	Spike	1220	FIAGLIAIV	HLA-B*46:01	0.102	-138.2	ILE-6, VAL-9
c	Spike	1220	FIAGLIAIV	HLA-C*03:04	0.100	-146.6	PHE-1, ALA-3, ILE-8, VAL-9
d	Envelop	4	FVSEETGTL	HLA-A*02:06	0.052	-147.7	PHE-1, VAL-2, SER-3, GLU-4, THR-6
e	Envelop	4	FVSEETGTL	HLA-B*46:01	0.102	-140.2	PHE-1, SER-3, GLU-4, THR-6, THR-8
f	Envelop	4	FVSEETGTL	HLA-C*07:02	0.152	-136.7	PHE-1, GLU-4, THR-8, LEU-9



bioRxiv preprint doi: <https://doi.org/10.1101/2020.03.03.962332>; this version posted March 3, 2020. The copyright holder for this preprint (which was not certified by peer review) is the author/funder. All rights reserved. No reuse allowed without permission.

Figure 1

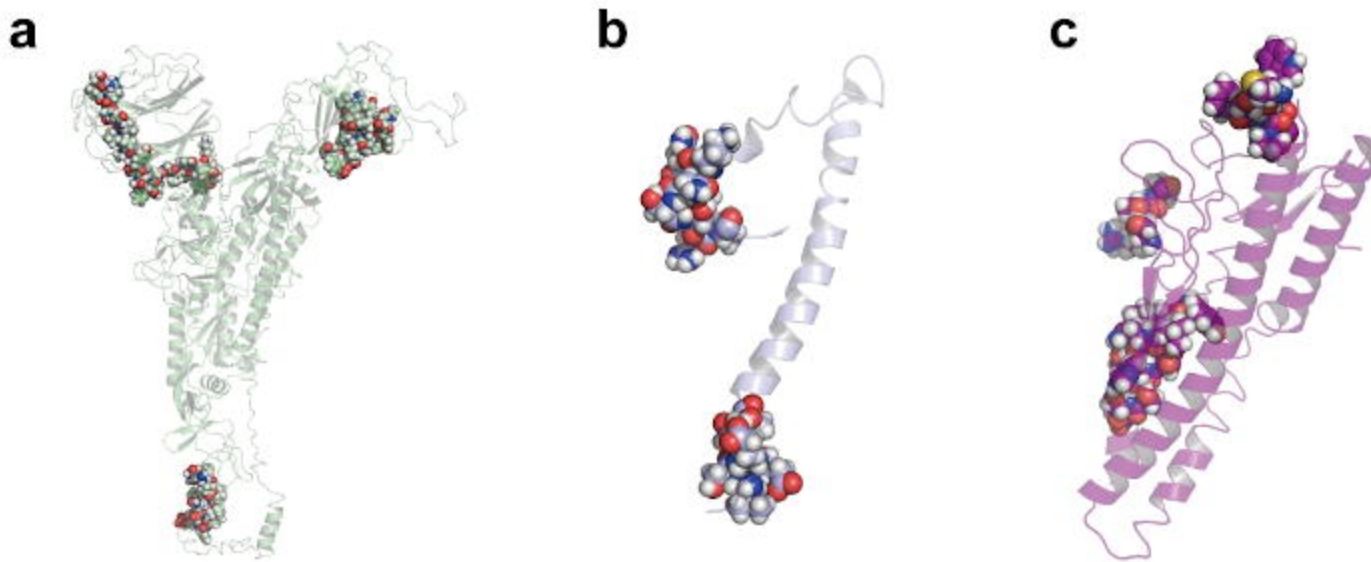


Figure 2

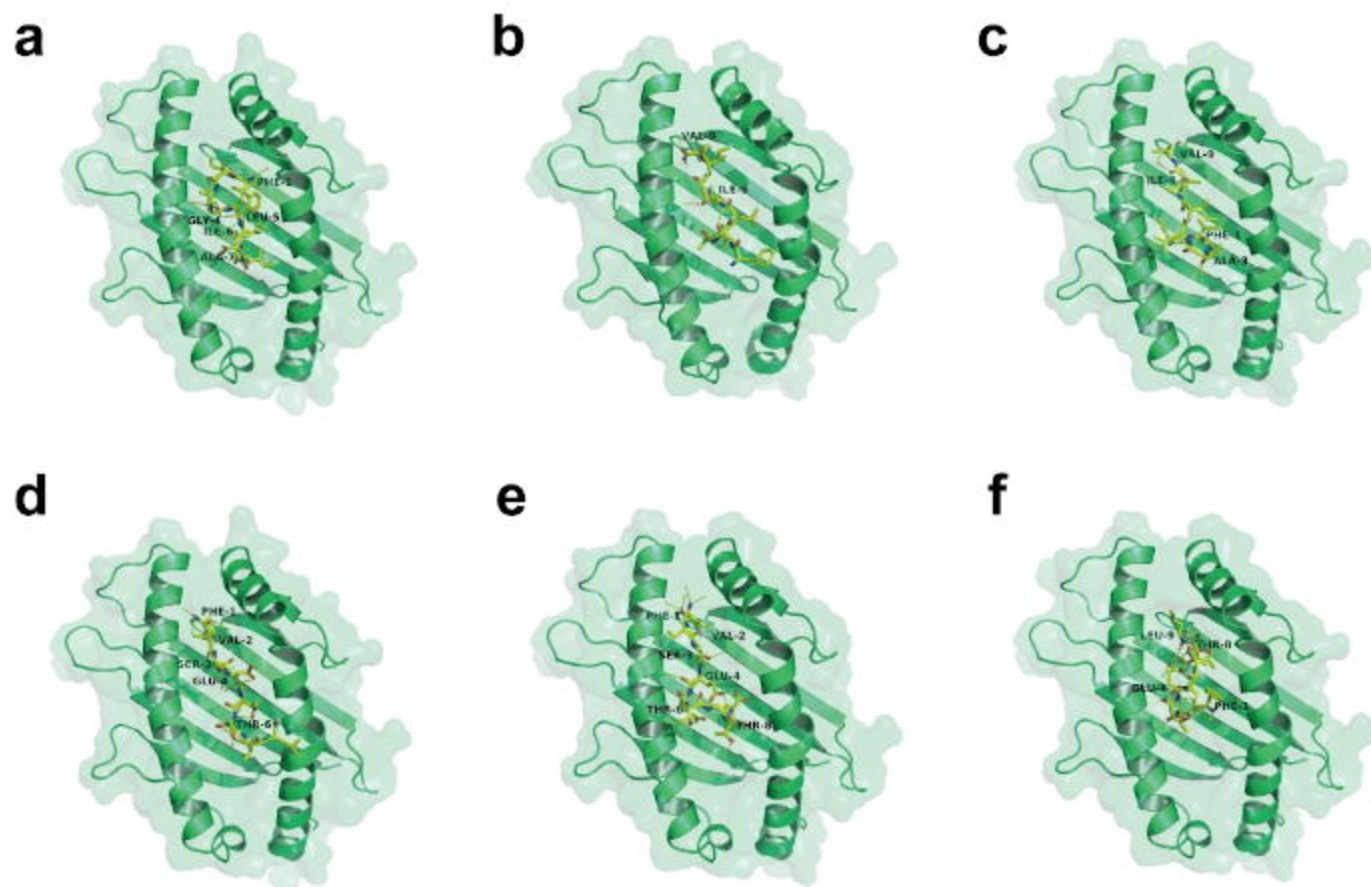


Figure 3